A Model for Optic Flow Integration in Locust Central-Complex Neurons Tuned to Head Direction

Kathrin Pabst[1], Frederick Zittrell[2],Uwe Homberg[2],Dominik Endres[1]
[1]Department of Psychology, Gutenbergstraße 18, 35032 Marburg, Germany
[2]Department of Biology, Karl-von-Frisch-Straße 8, 35043 Marburg, Germany
{kathrin.pabst, dominik.endres}@uni-marburg.de, {zittrell, homberg}@biologie.uni-marburg.de

Abstract

Navigation is a fundamental cognitive function of virtually all moving animals. Several navigation strategies require an estimate of the current traveling direction that is updated continuously. In the central complex of the insect brain, multimodal cues are fused into a compass-like head direction representation. Based on the proposed connectivity of columnar neurons in the central complex of the desert locust we designed a computational model to examine how these neurons could maintain a stable representation of heading direction and how shifts occur by optic flow signals when the animal turns. Our model differs from previous architectures in the excitation-inhibition interactions. Consequently, the activity of head direction-encoding CL1a neurons remains stable if it is mirrored by CL2 neurons, which are another class of columnar neurons. Shifts of the compass signal occur via modulation of the network connectivity. Our model can be used to deduce testable hypotheses where data are lacking, inspiring new avenues of experimental investigations.

Keywords: insect brain; central complex; sky compass orientation; optic flow; desert locust

Introduction

Animals display an abundance of navigational strategies allowing them to find their way in complex environments. Irrespective of the time frame and range of navigation behaviors, most of these strategies require a sense of the current relative heading direction (Heinze, 2017). Many insects, such as bees (von Frisch, 1946), ants (Fent, 1986), butterflies (Perez, Taylor, & Jander, 1997), and fruit flies (Weir & Dickinson, 2012), infer their traveling direction from celestial cues. A robust estimate emerges when celestial cues are combined with possibly redundant signals of other modalities (Honkanen, Adden, Freitas, & Heinze, 2019). We are interested in the computations involved in the maintenance of the animal's current heading direction.

Multimodal sensory inputs are processed in the central complex (CX), a prominent formation of neuropils that has emerged as the navigation hub of the insect brain (Green & Maimon, 2018; Honkanen et al., 2019; Pfeiffer & Homberg, 2014). It is characterized by a modular architecture with the protocerebral bridge (PB), the upper (CBU) and lower (CBL) divisions of the central body (CB, also termed ellipsoid and fan-shaped body in some species) being divided into columns, and the CB and paired noduli (NO) further divided into layers (Figure 1A; (Homberg, 2008; Pfeiffer & Homberg, 2014)). Columnar neurons interconnect the PB, CB, and the NO (Homberg, 2008). They arborize in PB and CB columns in a distinct projection pattern (Heinze & Homberg, 2008; Müller, Homberg, & Kühn, 1997; Wolff, Iyer, & Rubin, 2015) (see Figure 1B). Tangential neurons provide the CX with inputs from various brain regions. They innervate most or all columns of the PB or entire layers of the CB, some have additional arborizations in the NO (von Hadeln et al., 2020). Tangential neurons (SpsP in the fly, TB7 in the locust) from the posterior superior slope innervate one hemisphere of the PB and likely contact CL1a and CL2 neurons across the PB depending on turn direction, like SpsP neurons in the fly (von Hadeln et al., 2020; Green & Maimon, 2018; Lu et al., 2022).

CX neurons in various insect species respond to celestial cues (Homberg, Heinze, Pfeiffer, Kinoshita, & Jundi, 2011). In the locust they topographically map the solar azimuth (Pegel, Pfeiffer, Zittrell, Scholtyssek, & Homberg, 2019) and polarization pattern of the sky (Zittrell, Pfeiffer, & Homberg, 2020), giving rise to an internal sky compass (Figure 1B). In many insects, the CX features a representation of the current relative heading direction, in tune with external signals like sky compass cues or based solely on self- generated signals in their absence (Seelig & Jayaraman, 2015; Turner-Evans et al., 2017). Central place foragers like ants (Ronacher & Wehner, 1995) and bees (Srinivasan, Zhang, & Bidwell, 1997) rely on celestial cues for a sense of direction and on optic flow-based speed cues to estimate the traveled distance. Rotation-induced optic flow information could also be used for self-motion dependent direction updates when idiothetic sky signals are unavailable or noisy.

It has been shown that compass cell activity is modulated by visual motion in the locust (Rosner, Pegel, & Homberg, 2019). However, the neural circuitry performing optic flow integration in the CX remains largely unknown. Recently, computational models for angular path integration in the CX based on data from *Drosophila* and the sweat bee *Megalopta* have been proposed (Stone et al., 2017; Su, Lee, Huang, Wang, & Lo, 2017; Turner-Evans et al., 2020). We chose a similar approach to explore the connectivity of a subset of CX neurons involved in head direction encoding in the desert locust (*Schistocerca gregaria*) and computational mechanisms that produce sky compass-like characteristics. In the next section, we describe a neural firing rate model that respects known connectivity constraints from the locust and from the fruit fly (*Drosophila*) where locust data are missing. We first describe how the stereotypic projection pattern of columnar

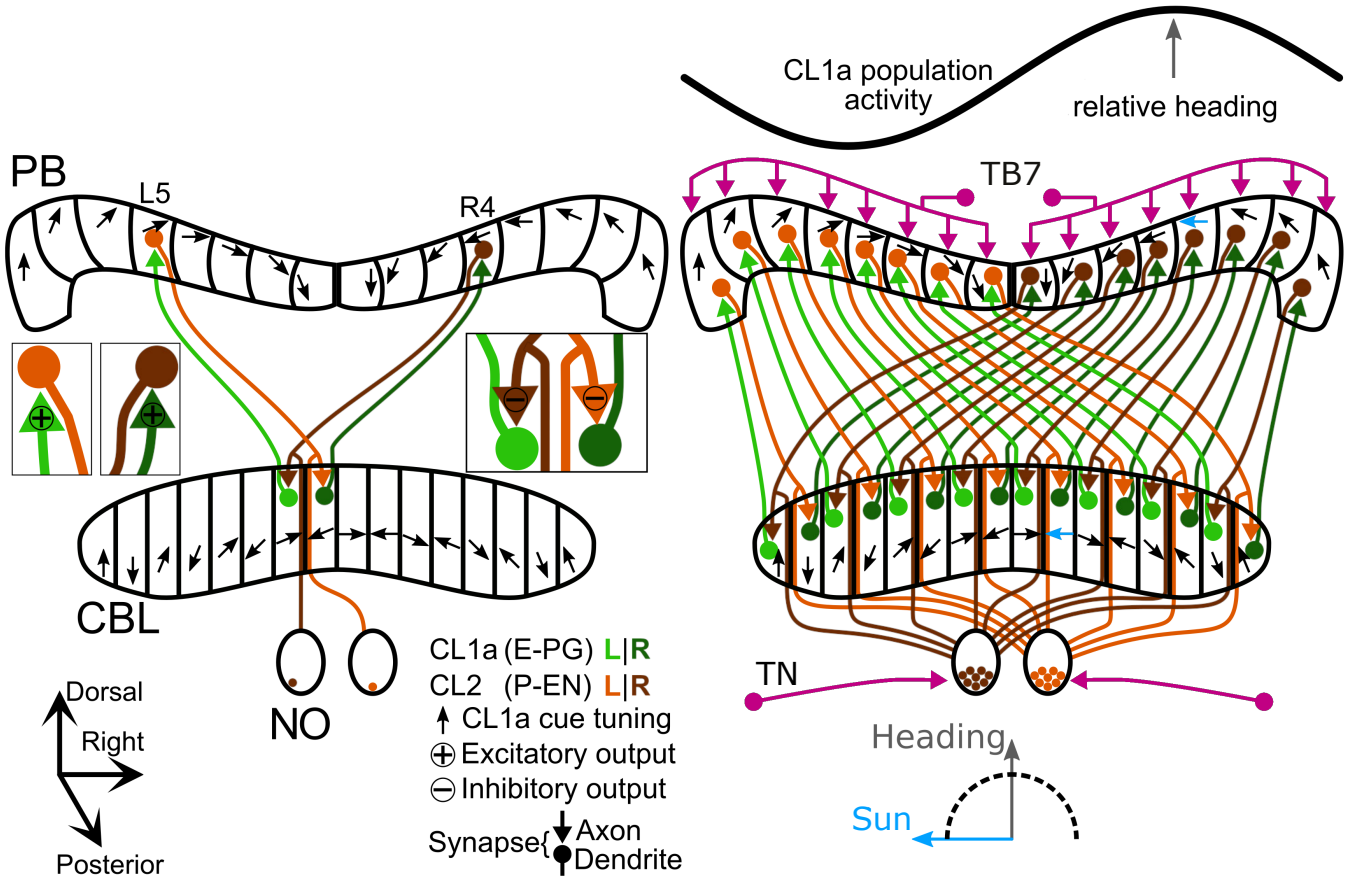

Figure 1: The abstracted connectivity diagram of the locust central complex, based on Heinze and Homberg (2008) and Zittrell et al. (2020). (A) Schematic of the CX with a subset of the involved neuron types: CL1a and CL2 neurons are connected to one another in the protocerebral bridge (PB) and lower division of the central body (CBL). CL2 neurons, in addition, have postsynaptic arborizations in the noduli (NO) where they receive possibly rotation-dependent input from tangential neurons (TN) from the lateral complexes. Rotation inputs may, likewise, be conveyed in the PB by tangential neurons (TB7) from the superior posterior slope. CL1a neurons are topographically tuned to solar azimuth along the PB (black arrows). Consequently, CL1a neurons with dendrites in adjacent columns of the CBL have 180° shifted tuning preference. (B) Full population of CL1a and CL2 neurons and CL1a activity pattern: With the sun 90° left of the locust (bottom), the CL1a population activity (top) has a distinct maximum according to their neural tuning (highlighted arrows in PB and CBL).

neurons can maintain stable head direction estimates when the locust stands still and then explore possible computational mechanisms that would update this internal representation during turns using optic flow-based rotation signals, presumably provided by TN and/or TB7 neurons. Finally, we discuss the ramifications of our work, comparing the locust network to that of the fly which has inspired previous models, and indicating where further research is needed to support our assumptions.

The Model

All computations were performed with the python programming language (version 3.8.5) and the pytorch library (version 1.10.0). Plots were created with the matplotlib library (version 3.3.2). The code is available in this repository.

Model Design

Our model entails a subset of the columnar neurons: CL1a neurons corresponding to E-PG neurons in the fly tracking head direction in the CX (Seelig & Jayaraman, 2015; Zittrell et al., 2020), and CL2 neurons corresponding to P-EN neurons responding to turning motion (Green et al., 2017; Turner-Evans et al., 2017; Zittrell et al., 2020).

We adopted the schemes proposed by Heinze and Homberg (2008) for the CL1a and CL2 connectivities. We hypothesized that, as shown for E-PG and P-EN neurons in the fly (Turner-Evans et al., 2017), CL1a neurons provide synaptic inputs to CL2 neurons in the PB, which in turn provide synaptic inputs to CL1a neurons in the CBL. Unlike Turner-Evans et al. (2017) who proposed a similar model for *Drosophila*, we do not assume excitatory connections in both sites paired with global inhibition, but instead a sign reversal

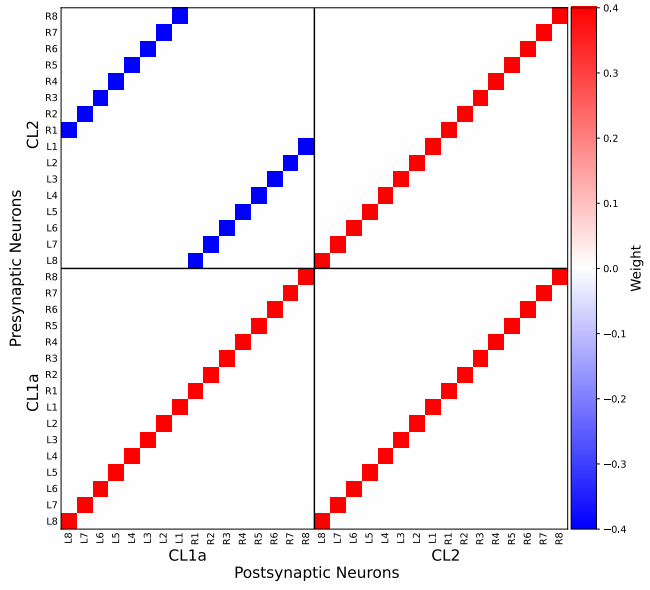

Figure 2: The connectivity matrix M derived from the wiring scheme in Figure 1A (upper left and lower right quadrants) with added excitatory self- recurrent connections (main diagonal).

within the CL1a-CL2 connectivity, presumably at the synapse in the CBL where inhibitory inputs could reverse the opposing tuning preference of CL1a neurons in neighboring CBL columns otherwise resulting from the connectivity (see Figure 1). Based on these assumptions, we constructed a connectivity matrix M. For modeling purposes, we added excitatory self-recurrent connections to all neurons to enable them to maintain a baseline activity. Note that the self-recurrent connections are not a faithful representation of the known neuroarchitecture. Other mechanisms of activity maintenance, e.g., loops across several neurons or change of membrane properties, are conceivable too, and have been implemented in previous models. We chose self- recurrent loops for our model because they comprise the simplest solution, and we have no data from the locust that require otherwise. We assigned uniform weights to all excitatory and inhibitory connections, 0.5 and -0.5, respectively. We made this choice to obtain eigenvalues equal to one, see next section for details. See Figure 2 for a visualization of M.

We employed a discrete time framework where the activity deviation of all neurons from their baseline at time t is represented by a vector x_t with components $x_{t,1:16}$ and $x_{t,17:32}$ covering the CL1a and CL2 neurons, respectively. We assume only small deviations, hence we can use a linear network as an approximation to non-linear dynamics. The network is recurrent and iterated across time steps such that the activity at the next time step can be computed from the current activity:

$$x_{t+1} = Mx_t. \tag{1}$$

Maintenance of a Stable Head Direction Encoding

We first set out to test whether the proposed network could maintain a stable head direction encoding in the CL1a activity.

Methods In the framework outlined above, maintenance of the head direction representation or CL1a activity pattern $x_{1:16}$ translates to an equality of $x_{t_{1:16}}$ at time point t and $x_{t+1_{1:16}}$ at the following time point, $t+1$:

$$x_{t_{1:16}} = x_{t+1_{1:16}}. \tag{2}$$

According to equation 1, this is given if $Mx_t = x_t$. This equality holds for all x_t that are eigenvectors u of M where $\delta_r = 1$, with δ_r denoting the real part of the corresponding eigenvalue, and zero imaginary part. We refer to these eigenvectors as 'stable'. Therefore, any linear combination of these stable eigenvectors will be a stable state of the network, too. We tested whether any of these stable states resembled activity observed in the locust CX. Based on the $1 \times 360°$ compass topography reported in the locust PB (Pegel et al., 2019; Zittrell et al., 2020) (see Figure 1), we defined $n = 1 \ldots 16$ different CL1a activity targets $\hat{x}$, each with the maximum in a different column:

$$\hat{X}^n_{t+1_{1:16}} = cos(\vec{\phi}_{CL1a} + n\vec{\phi}) / \|cos(\vec{\phi}_{CL1a} + n\vec{\phi})\|_F. \tag{3}$$

where $\hat{X}$ is a matrix containing all $\hat{x}$ and $\|\|_F$ denotes the Frobenius norm. $\vec{\phi}_{CL1a}$ is the vector of preferred azimuths of the CL1a neurons, approximated to be evenly distributed across the PB from left to right in a range $[0, 2\pi]$, $\vec{\phi} = (\phi \ldots \phi)$ with $\vec{\phi} = \frac{2\pi}{16}$, the angle covered by a PB column (see Figure 1). These activity targets are thus cosine-shaped across the PB with the maximum and minimum 8 columns apart (see Fig. 1B). Note that all activities should be understood as firing rate differences to a baseline firing rate. To find the linear coefficient vectors a which result in CL1a activities equal to the target CL1a activities (see equation 3), we employed the L-BFGS algorithm to optimize A, a matrix comprising all a, with respect to a loss function

$$L = \|(U_{\lambda_r=1}A)_{1:16} - \hat{X}_{t+1_{1:16}}\|^2_F + 0.1\|A\|_F, \tag{4}$$

where $U_{\lambda_r=1}$ is the matrix of stable eigenvectors sorted by $\|\lambda\|_F$, the Frobenius norm of the real and imaginary parts of the corresponding λ. The first term of this loss function measures the divergence of the CL1a activations from the targets, the second term regularizes the solution: of all A that represent a given target state, the optimizer picks the one that minimizes the length of A, thus avoiding solutions where contributions from different eigenvectors cancel each other. Optimization was iterated until convergence to four digits. We tested whether the maintenance criterion was fulfilled;

$$[M(U_{\lambda_r=1}A)]_{1:16} = (U_{\lambda_r=1}A)_{1:16}. \tag{5}$$

Results A matrix A of coefficient vectors for the linear combination of stable eigenvectors $U_{\lambda=1}$ was found that reproduced $\hat{X}$ up to machine precision. The optimization process

employed here always converged at $U_{\lambda=1}A_{1:16} = U_{\lambda=1}A_{17:32}$ (see Figure 3A: Three targets $\hat{x}$ (solid lines) along with the matching activities x resulting from the optimization (dots) are exemplarily shown in different colors). In other words, with our proposed model and CL1a activity targets, when the latter are stable head direction estimates, the CL2 activation patterns are exactly the same; $x_{t+1,1:16} = x_{t,1:16}$ if $x_{t,1:16} = x_{t,17:32}$.

Rotation-induced Shifts of Compass Activity

An internal compass representation must adapt to a new heading direction when the animal turns. In the fly, it has been observed that the compass activity bump shifts counter- phasic to the turn, i.e., such that the activity pattern signals a fixed allocentric direction (Giraldo et al., 2018; Seelig & Jayaraman, 2015). We therefore investigated how the stable CL1a activation patterns of our model would be shifted in the opposite direction of the animal's turn direction by an input representing optic flow information. We hypothesize that such an input could be mediated by TN and TB7 neurons as they supply the CX with various inputs. Furthermore, in Drosophila, their counterparts (LNO and SpsP neurons) have been shown to respond to turning motion (Lu et al., 2022).

Methods We conceptualized such shifts as switches between consecutive time points t and $t+1$ from one of the activation patterns to another, with the activity maximum moving to the nearest neighboring PB column, i.e., the yaw angle is always $\pm\frac{2\pi}{16}$. We thus searched for a computational mechanism that would produce, starting at x_t^n, $x_{t+1}^n = x_t^{n-1}$ for left turns and $x_{t+1}^n = x_t^{n+1}$ for right turns. Note that we expect $x_{t,1:16} = x_{t,17:32}$ at all times t even though an offset between E-PG and P-EN peak activity has been observed during turns in flies (Turner-Evans et al., 2017). This is due to the discrete time framework employed here where the dynamics of transitions between time points are not made explicit. We explored two different ways of changing the network's activity x: An additive feed forward input exciting or inhibiting the CL1a and CL2 neurons, and a multiplicative input effect modulating the network's synaptic weights M. To test whether an additive effect could produce these shifts, we optimized two vectors y^L and y^R to minimize

$$L = \|[M\hat{X}_t + y^L] - \hat{X}_{t+1}^L\|_F^2 + 0.1\|y^L\|_F \tag{6}$$

and

$$L = \|[M\hat{X}_t + y^R] - \hat{X}_{t+1}^R\|_F^2 + 0.1\|y^R\|_F \tag{7}$$

for left and right turns of the animal resulting in right and left shifts of the activity pattern, respectively. Here, $\hat{X}_{t+1}^{L,1} = \hat{X}_{t+1}^{32}$ and $\hat{X}_{t+1}^{L,2:32} = \hat{X}_{t+1}^{1:31}$, and $\hat{X}_{t+1}^{R,1:31} = \hat{X}_{t+1}^{2:32}$ and $\hat{X}_{t+1}^{R,32} = \hat{X}_{t+1}^{1}$; i.e., $\hat{X}_{t+1}^L$ and $\hat{X}_{t+1}^R$ are the activation pattern targets learned in the maintenance experiment described above shifted one position to the right and left, respectively. Note that the superscript specifies the animal's turn direction.

To test whether a modulatory input could yield the desired shifts, we optimized matrices Y^L and Y^R to minimize

$$L = \|[M_s Y^L \hat{X}_t] - \hat{X}_{t+1}^L\|_F^2 + 0.1\|Y^L\|_F \tag{8}$$

and

$$L = \|[M_s Y^R \hat{X}_t] - \hat{X}_{t+1}^R\|_F^2 + 0.1\|Y^R\|_F, \tag{9}$$

where M_s denotes M convolved with an RBF Kernel with kernel width of 1 column, in other words a smoothed version of the connectivity matrix, corresponding to broader arborizations (see Figure 3B). This way, the modulatory input can manipulate any connection existing in M but also add connections, with their possible strength decreasing with their distance to existing connections. This approach was chosen since a modulation of only the connections indicated by the wiring scheme (see Fig. 1) and present in M could not yield the desired shift results. The smoothed matrix was inspired by the E-PN and P-EG connectivity reported in *Drosophila* (Hulse et al., 2021). In the locust, arborizations of CL2 neurons in the CBL are confined to single columns, while those of CL1 neurons usually extend across at least three columns (Heinze & Homberg, 2008). Optimization was iterated until convergence to four digits.

Results No vectors y^L and y^R could be found that would produce the desired phase shift to the right or left for all x^n. Optimization converged at $X_{t+1} = X_t$ (see Figure 3C and C': Three initial states x_t (dashed lines) and the matching target states $\hat{x}_{t+1}$ (solid lines) along with the activities x_{t+1} resulting from the optimization (dots) are exemplarily shown in different colors). This demonstrates that purely feed forward input to the CL1a/CL2 neurons cannot account for the observed shift behavior. Instead, we found two matrices Y^L and Y^R that would move any of the 16 predefined activation patterns to the right or left (see Figure 3D and D': As in 3C and C', three matching initial, target, and trained activity states are shown). In both modulated matrices, activity is suppressed in adjacent columns on one but increased in the ones on the other side in addition to the existing connections, thereby effecting a shift of the activation pattern (see Figure 3E and E').

Discussion

As the computational mechanisms underlying the locust sky compass are largely unknown, we constructed a simplified model of the columnar neurons of the locust central complex to explore the circuit on the algorithmic level of analysis, in the sense of Marr and Poggio (1979).

Constrained by available physiological and anatomical data, we built a computational model of CX neurons in the locust capable of maintaining and shifting a stable head direction representation. Where no locust data was available, our model was inspired by data from the fruit fly, leading to a resemblance to models for angular velocity integration in the *Drosophila* CX compass (Kakaria & De Bivort, 2017; Turner-Evans et al., 2017; Pisokas, Heinze, & Webb, 2020; Turner-Evans et al., 2020; Hulse et al., 2021). Key differences however are the $1 \times 360°$ angular representation in the locust

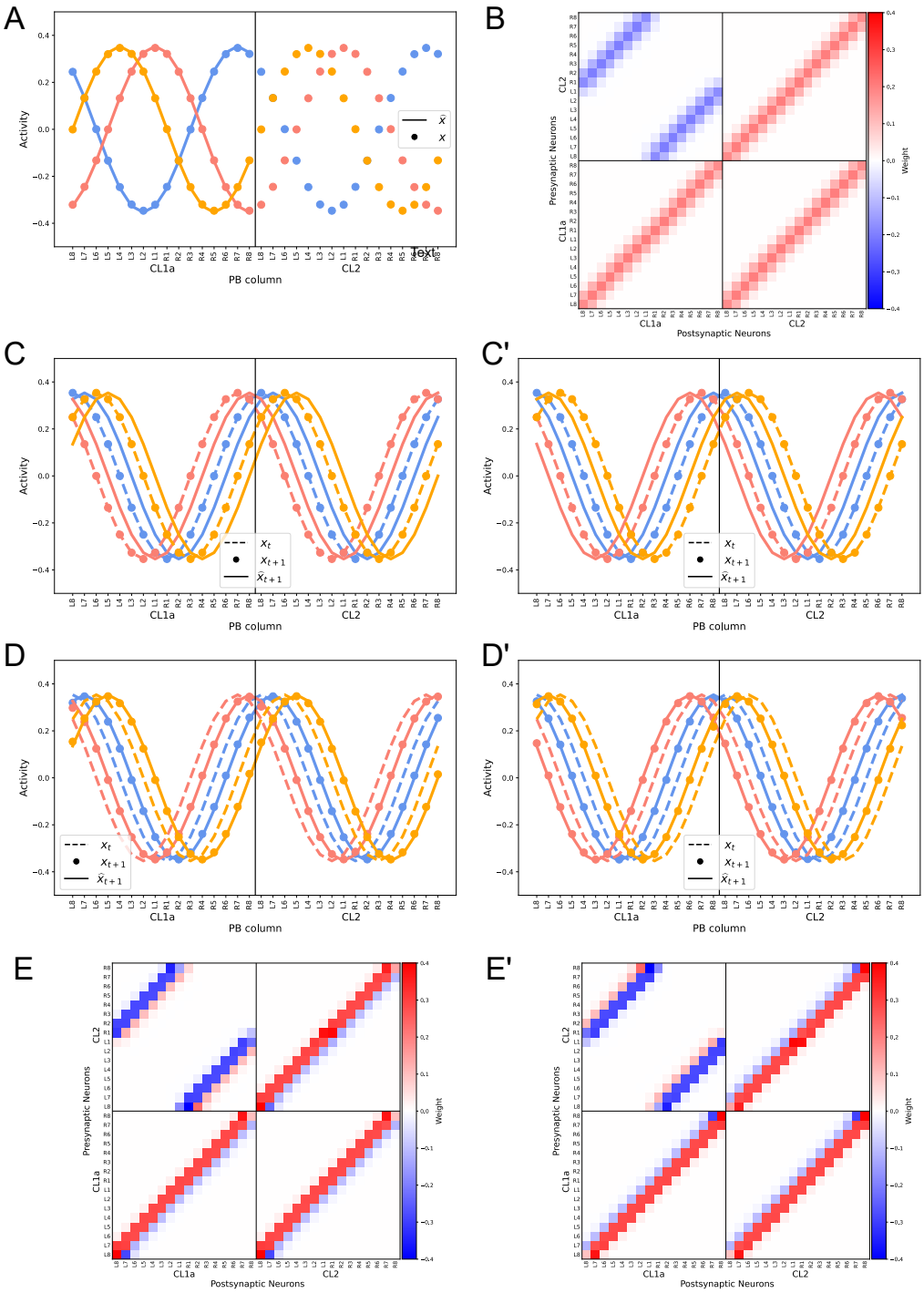

Figure 3: Modeling results. (A) When CL1a activities $x_{1:16}$ (dots) converge with CL1a activity targets $\hat{x}_{1:16}$ (solid lines), CL1a and CL2 activity are equal. As shown for three different pairs of x and $\hat{x}$. (B) The smoothed matrix M_s, which we used to derive the connectivity matrix for rotational movements. (C) No feed forward input y^L could be found that would shift the initial activity x_t (dashed lines) to the target activity $\hat{x}_{t+1}$ (solid lines). $x_{t+1} = x_t + y^L$ (dots) does not differ from x_t. Three examples are shown in different colors. (C") Likewise, no y^R could be found that would shift the activity to the left. (D) A modulatory input Y^L produces the targeted activity shift to the right. (D') Likewise, modulation by Y^R causes a transition to the left. (E) Y^L, the modulated connectivity matrix causing a shift to the right. (E') Y^R, the modulated connectivity matrix causing a shift to the left.

PB (Pegel et al., 2019; Zittrell et al., 2020) compared to the $2 \times 360°$ representation of space in the *Drosophila* PB and, contrasting the excitatory E-PG/P-EN loops in the fly, the assumed inhibitory synapses from CL2 onto CL1a neurons in the CBL which need to be supported by future physiological analyses.

Our model maintains a stable CL1a head direction encoding if the CL1a and CL2 activity are identical. This is in line with the minimal offsets between the E-PG and P-EN activity bumps observed in fruit flies walking in darkness at angular velocities below 30°/s (Turner-Evans et al., 2017). On the other hand, equal CL1a and CL2 activities are not in line with different responses of CL1a and CL2 neurons to polarized light as reported by (Heinze & Homberg, n.d.). This could be accounted for by adjusting the network weights in future versions of our model. Future models could also explore how properties of the network depend on context and available cues.

We investigated two different ways of shifting the CL1a compass activity, presumably mediated by TN and/or TB7 neurons in the locust. In our model, an additive or feed forward input to the CL1a and CL2 neurons could not reproduce the shift of activity observed in the CX. The locust model proposed by Pisokas et al. (2020), in contrast, shifts the compass bump via excitation of P-EN (CL2) neurons in one hemisphere, and inhibition of those in the other, depending on the turn direction. This is in line with the P-EN responses of fruit flies walking in darkness reported by Turner-Evans et al. (2017). Our model, however, would require connections between CL2 and CL1a neurons in the same column to shift the compass activity via this mechanism. Comparable connections exist between rotation- and head direction cells in the model of the rat's internal compass proposed by Skaggs, Knierim, Kudrimoti, and McNaughton (1994). Skaggs et al. further assume that the weights of synapses from visual feature detectors - cells that respond to relative positions of stimuli such as landmarks or the sun - on head direction cells are modulated by the firing rate of the latter. In our model, too, a multiplicative or modulatory effect of rotation input on the CL1a/CL2 connectivity successfully shifts the activity pattern to the left or right. We originally assumed a connectivity based on single column innervations of each neuron, and this was sufficient for the maintenance of a compass signal. The compass shift, however, requires CL1a and CL2 neurons exciting and inhibiting each other in three adjacent columns. Likewise, it requires connections among neighboring CL1a neurons and among neighboring CL2 neurons, respectively. Substantial overlap of ramifications across columns has been observed for CL1a neurons in the CBL of the locust (Heinze & Homberg, 2008), but whether connections actually exist among CL1a and CL2 neurons, respectively, and between CL2- and CL1a neurons of neighboring columns requires further research. Furthermore, it needs to be examined how the proposed modulation could act in a turn direction-dependent manner and how rotation cues of different modalities, such as optic flow, proprioceptive feedback, or efferent copies are processed and integrated in the CX.

The linear model and binary concept of movement employed here are abstractions of the neuronal and behavioral characteristics of the locust. In particular, our model has time-discrete dynamics; it switches between activity states and does not make the dynamics driving the transitions explicit. This means that it cannot model a spatiotemporal relationship between the CL1a and CL2 neurons like the lead-lag relationship between E-PG and P-EN observed by Turner-Evans et al. (2017) in the fly. Furthermore, our model is a single compartment model, meaning that each neuron is assigned one activity. Thus, a phenomenon like the reversal of the lead-lag relationship of E-PG and P-EN between the PB and EB reported by the same authors cannot be exhibited in our model. We aim to increase the model's biological plausibility by implementing velocity dependence in future work but expect the general principles of maintaining and updating the compass bump to hold independently of the level of analysis. Nevertheless, it will be interesting to consider sources of non-linearity in neural signal processing and transmission. The locust model proposed by Pisokas et al. (2020) is noise tolerant and the authors attribute this to recurrent connections. We aim to test if the same applies to our model. We further intend to explore if the integration of rotation information from different sources can increase the robustness of the compass signaling and how the compass responds to contradictory inputs from different modalities.

Acknowledgements

This work was supported by the DFG (452193090, HO 950/28-1, and EN 1152/3-1) and "The Adaptive Mind", funded by the Excellence Program of the Hessian Ministry for Science and the Arts.

References

Fent, K. (1986). Polarized skylight orientation in the desert ant cataglyphis. *Journal of Comparative Physiology A*, *158*, 145-150.

Giraldo, Y. M., Leitch, K. J., Ros, I. G., Warren, T. L., Weir, P. T., & Dickinson, M. H. (2018). Sun navigation requires compass neurons in drosophila. *Current Biology*, *28*, 2845-2852. doi: 10.1016, j.cub.2018.07.002

Green, J., Adachi, A., Shah, K. K., Hirokawa, J. D., Magani, P. S., & Maimon, G. (2017). A neural circuit architecture for angular integration in drosophila. *Nature*, *546*, 101-106. doi: 10.1038, nature22343

Green, J., & Maimon, G. (2018). Building a heading signal from anatomically defined neuron types in the drosophila central complex. *Current Opinion in Neurobiology*, *52*, 156–164. doi: 10.1016, j.conb.2018.06.010

Heinze, S. (2017). Unraveling the neural basis of insect navigation. *Current Opinion in Insect Science*, *24*, 58-67. doi: 10.1016, j.cois.2017.09.001

Heinze, S., & Homberg, U. (n.d.). Linking the input to the output: new sets of neurons complement the polarization vision network in the locust central complex. doi: 10.1523, JNEUROSCI.0332-09.2009

Heinze, S., & Homberg, U. (2008). Neuroarchitecture of the central complex of the desert locust: Intrinsic and columnar neurons. *Journal of Comparative Neurology*, *511*, 454-478. doi: 10.1002, cne.21842

Homberg, U. (2008). Evolution of the central complex in the arthropod brain with respect to the visual system. *Arthropod Structure and Development*, *37*, 680-687. doi: 10.1016, j.asd.2008.01.008

Homberg, U., Heinze, S., Pfeiffer, K., Kinoshita, M., & Jundi, B. E. (2011). Central neural coding of sky polarization in insects. *Philosophical Transactions of the Royal Society B: Biological Sciences*, *366*, 680-687. doi: 10.1098, rstb.2010.0199

Honkanen, A., Adden, A., Freitas, J. D. S., & Heinze, S. (2019). The insect central complex and the neural basis of navigational strategies. *Journal of Experimental Biology*, *222*. doi: 10.1242, jeb.188854

Hulse, B. K., Haberkern, H., Franconville, R., Turner-Evans, D. B., Takemura, S. Y., Wolff, T., ... Jayaraman, V. (2021). A connectome of the drosophila central complex reveals network motifs suitable for flexible navigation and context-dependent action selection. *eLife*, *10*. doi: 10.7554, eLife.66039

Kakaria, K. S., & De Bivort, B. L. (2017). Ring attractor dynamics emerge from a spiking model of the entire protocerebral bridge. *Frontiers in Behavioral Neuroscience*, *11*, 8.

Lu, J., Behbahani, A. H., Hamburg, L., Westeinde, E. A., Dawson, P. M., Lyu, C., ... Wilson, R. I. (2022). Transforming representations of movement from body- to world-centric space. *Nature*, *601*, 98-104. doi: 10.1038, s41586-021-04191-x

Marr, D., & Poggio, T. (1979). A computational theory of human stereo vision. *Proceedings of the Royal Society of London. Series B. Biological Sciences*, *204*(1156), 301–328.

Müller, M., Homberg, U., & Kühn, A. (1997). Neuroarchitecture of the lower division of the central body in the brain of the locust (Schistocerca gregaria). *Cell and Tissue Research*, *288*, 159-176. doi: 10.1007, s004410050803

Pegel, U., Pfeiffer, K., Zittrell, F., Scholtyssek, C., & Homberg, U. (2019). Two compasses in the central complex of the locust brain. *Journal of Neuroscience*, *39*, 3070-3080. doi: 10.1523, JNEUROSCI.0940-18.2019

Perez, S. M., Taylor, O. R., & Jander, R. (1997). A sun compass in monarch butterflies. *Nature*, *387*, 29. doi: 10.1038, 387029a0

Pfeiffer, K., & Homberg, U. (2014). Organization and functional roles of the central complex in the insect brain. *Annual Review of Entomology*, *59*, 165-184. doi: 10.1146, annurev-ento-011613-162031

Pisokas, I., Heinze, S., & Webb, B. (2020). The head direction circuit of two insect species. *Elife*, *9*, e53985.

Ronacher, B., & Wehner, R. (1995). Desert ants cataglyphis fortis use self-induced optic flow to measure distances travelled. *Journal of Comparative Physiology A*, *177*, 21-27. doi: 10.1007, BF00243395

Rosner, R., Pegel, U., & Homberg, U. (2019). Responses of compass neurons in the locust brain to visual motion and leg motor activity. *Journal of Experimental Biology*, *222*. doi: 10.1242, jeb.196261

Seelig, J. D., & Jayaraman, V. (2015). Neural dynamics for landmark orientation and angular path integration. *Nature*, *521*, 186-191. doi: 10.1038, nature14446

Skaggs, W., Knierim, J., Kudrimoti, H., & McNaughton, B. (1994). A model of the neural basis of the rat's sense of direction. *Advances in Neural Information Processing Systems*, *7*, 173-180.

Srinivasan, M. V., Zhang, S. W., & Bidwell, N. J. (1997). Visually mediated odometry in honeybees. *Journal of Experimental Biology*, *200*, 2513-2522. doi: 10.1242, jeb.200.19.2513

Stone, T., Webb, B., Adden, A., Weddig, N. B., Honkanen, A., Templin, R., ... Heinze, S. (2017). An anatomically constrained model for path integration in the bee brain. *Current Biology*, *27*, 3069-3085. doi: 10.1016, j.cub.2017.08.052

Su, T. S., Lee, W. J., Huang, Y. C., Wang, C. T., & Lo, C. C. (2017). Coupled symmetric and asymmetric circuits underlying spatial orientation in fruit flies. *Nature Communications*, *8*, 1-15. doi: 10.1038, s41467-017-00191-6

Turner-Evans, D. B., Jensen, K. T., Ali, S., Paterson, T., Sheridan, A., Ray, R. P., ... Jayaraman, V. (2020). The neuroanatomical ultrastructure and function of a biological ring attractor. *Neuron*, *108*, 145-163. doi: 10.1016, j.neuron.2020.08.006

Turner-Evans, D. B., Wegener, S., Rouault, H., Franconville, R., Wolff, T., Seelig, J. D., ... Jayaraman, V. (2017). An-

gular velocity integration in a fly heading circuit. *eLife*, *6*. doi: 10.7554, eLife.23496, e23496

von Frisch, K. (1946). Die Tänze der Bienen. *Österreichische Zoologische Zeitschrift*, *1*, 1-48.

von Hadeln, J., Hensgen, R., Bockhorst, T., Rosner, R., Heidasch, R., Pegel, U., ... Homberg, U. (2020). Neuroarchitecture of the central complex of the desert locust: Tangential neurons. *Journal of Comparative Neurology*, *528*, 906-934. doi: 10.1002, cne.24796

Weir, P. T., & Dickinson, M. H. (2012). Flying Drosophila orient to sky polarization. *Current Biology*, *22*(1), 21-27.

Wolff, T., Iyer, N. A., & Rubin, G. M. (2015). Neuroarchitecture and neuroanatomy of the drosophila central complex: A GAL4-based dissection of protocerebral bridge neurons and circuits. *Journal of Comparative Neurology*, *523*, 887-1037. doi: 10.1002, cne.23705

Zittrell, F., Pfeiffer, K., & Homberg, U. (2020). Matched-filter coding of sky polarization results in an internal sun compass in the brain of the desert locust. *Proceedings of the National Academy of Sciences of the United States of America*, *117*, 25810-25817. doi: 10.1073, pnas.2005192117